Scatterometer Winds Explain Damped Rossby Waves

Kathryn A. Kelly
Applied Physics Laboratory
University of Washington
kkelly@apl.washington.edu

LuAnne Thompson
School of Oceanography
University of Washington
luanne@ocean.washington.edu

Abstract

Westward propagating waves in the North Pacific Ocean are overwhelmed by a zonally coherent response in the latitude band 10-16˚N, as observed in sea surface height (SSH) anomalies from the TOPEX/POSEIDON altimeter. The apparent lack of wave propagation in this region has also been observed in anomalies in the oceanic thermocline (Kessler, 1990). SSH anomalies from a simple model of wave propagation, forced with two different wind products, is compared with the SSH expected from the seasonal heating cycle to understand the processes responsible for the coherent annual period signal. Based on three different flux products the seasonal heating cycle is out-of-phase and too small to be responsible for the observed annual cycle in SSH. Comparisons of wind-forced SSH forced by NCEP reanalysis winds and by winds from the QuikSCAT/SeaWinds scatterometer demonstrate that the observed SSH variations reflect the dominant local Ekman pumping response to zonally coherent wind stress that is produced only by the scatterometer fields. Rossby waves do propagate westward, but the magnitude of the free wave is smaller than the locally forced response. The wind stress variations are associated with the annual migration of the Intertropical Convergence Zone, which is not reproduced well by the NCEP model.

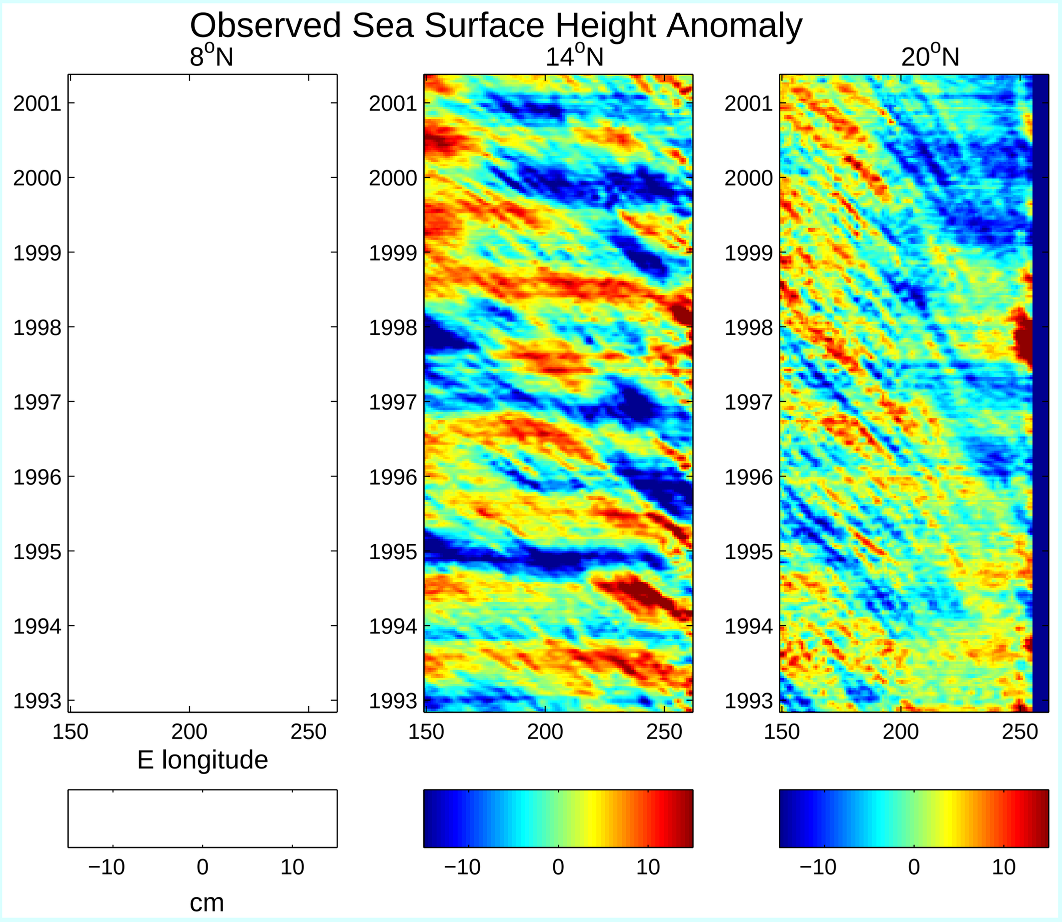

Figure 1. Time-longitude plots of SSH anomalies at (a) 8, (b) 14, and (c) 20˚N from the TOPEX/POSEIDON altimeter. Units are meters. Note the intermittent signal of the propagating Rossby waves at 14˚N, which is suggestive of a damping mechanism.

Models of SSH Anomalies

1) **Steric Response** to Surface Heating (Gill and Niiler 1973, Stammer 1997)

$$\boxed{\frac{\partial\eta}{\partial t} = \frac{\alpha_T \cdot Q_{net}}{\rho c_p}} \qquad (1)$$

where η = sea surface height anomaly,
α_T = coefficient of thermal expansion, and
Q_{net} = net surface heat flux.

2) Wind Forced **Rossby Waves** (Meyers, 1979)

$$\frac{\partial}{\partial t}(h - \lambda^2\nabla^2 h) - \beta\lambda^2\frac{\partial h}{\partial x} = curl\left(\frac{\vec{\tau}}{\rho_0 f}\right) \qquad (2a)$$

where h = thermocline depth anomaly,
$\lambda^2 = g'H/f^2$,
H=mean thermocline depth,
$g'=g\Delta\rho/\rho_0$, and
τ = wind stress.

Substituting $g'h = -g\eta$ yields an equation in η:

$$\boxed{\frac{\partial\eta}{\partial t} - \beta\lambda^2\frac{\partial\eta}{\partial x} = -\frac{g'}{gf\rho_0}curl\vec{\tau}} \qquad (2b)$$

Steric Response to Surface Heating

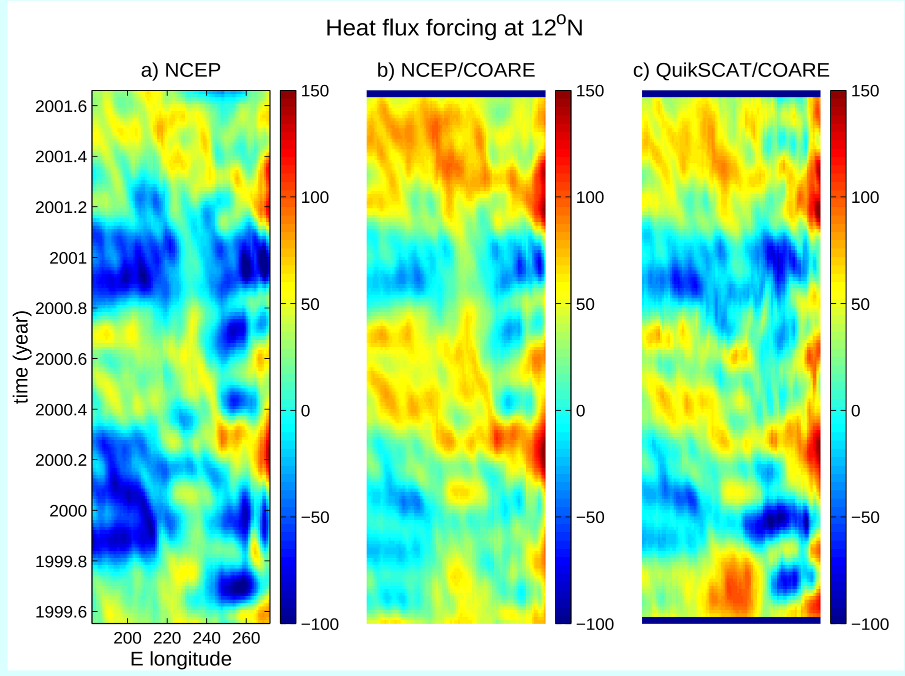

Figure 2. Net surface heat fluxes from (a) NCEP Reanalysis, (b) NCEP variables used in COARE bulk formulas, and (c) same as (b), except NCEP winds replaced by QuikSCAT winds in COARE algorithm.Units are Wm^{-2}.

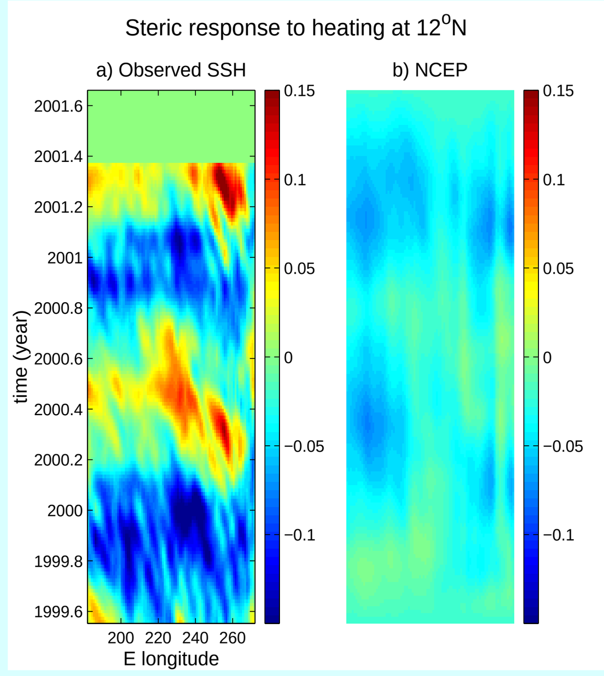

Figure 3. Observed and modeled SSH. (a) SSH anomalies from the altimeter, (b) thermal expansion anomalies from NCEP/COARE heat fluxes. Units are meters. The steric response to surface fluxes, for all three flux products, is out-of-phase and too small to explain the observed SSH anomalies.

Wind Forced Rossby Waves

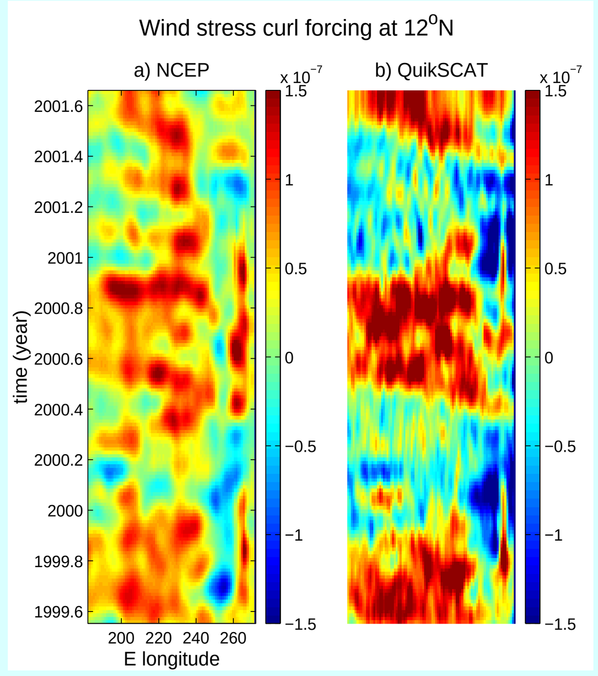

Figure 4. The wind stress curl as a function of time and longitude at 12˚N. Units are 10^{-7} N m^{-3} for (a) NCEP and (b) QuikSCAT. QuikSCAT curl has a more pronounced annual cycle that reflects the annual migration of the ITCZ.

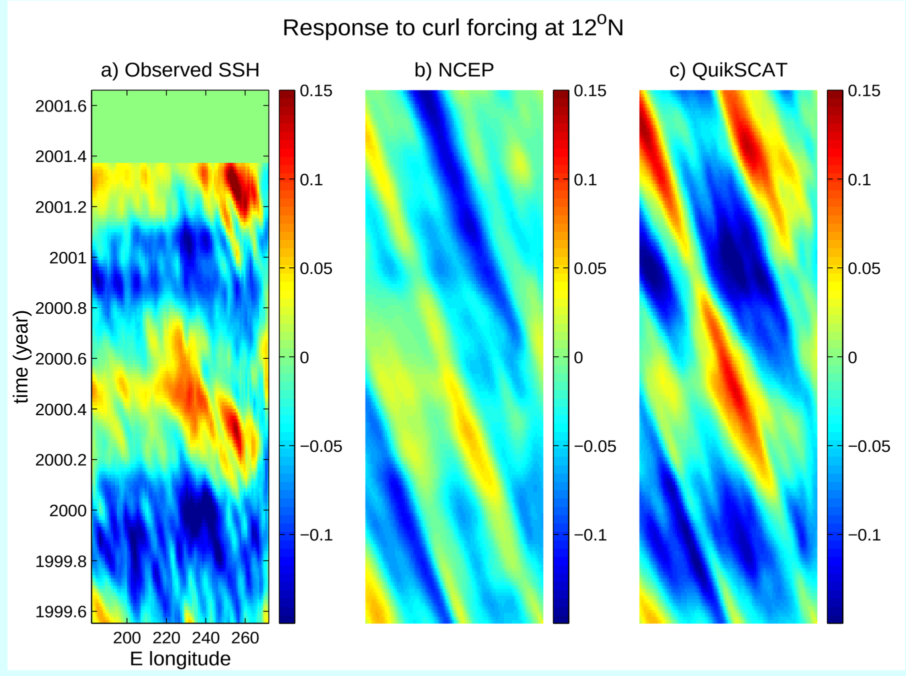

Figure 5. Observed SSH and SSH response to curl forcing. (a) SSH anomalies from the altimeter, (b) SSH anomalies when forced by NCEP Reanalysis winds, and (c), same as (b), except forced by QuikSCAT winds. The NCEP curl produces an SSH anomaly field dominated by propagating waves. QuikSCAT curl produces a strong local response with a pronounced annual cycle that tends to obscure the propagation, similar to the observed SSH.

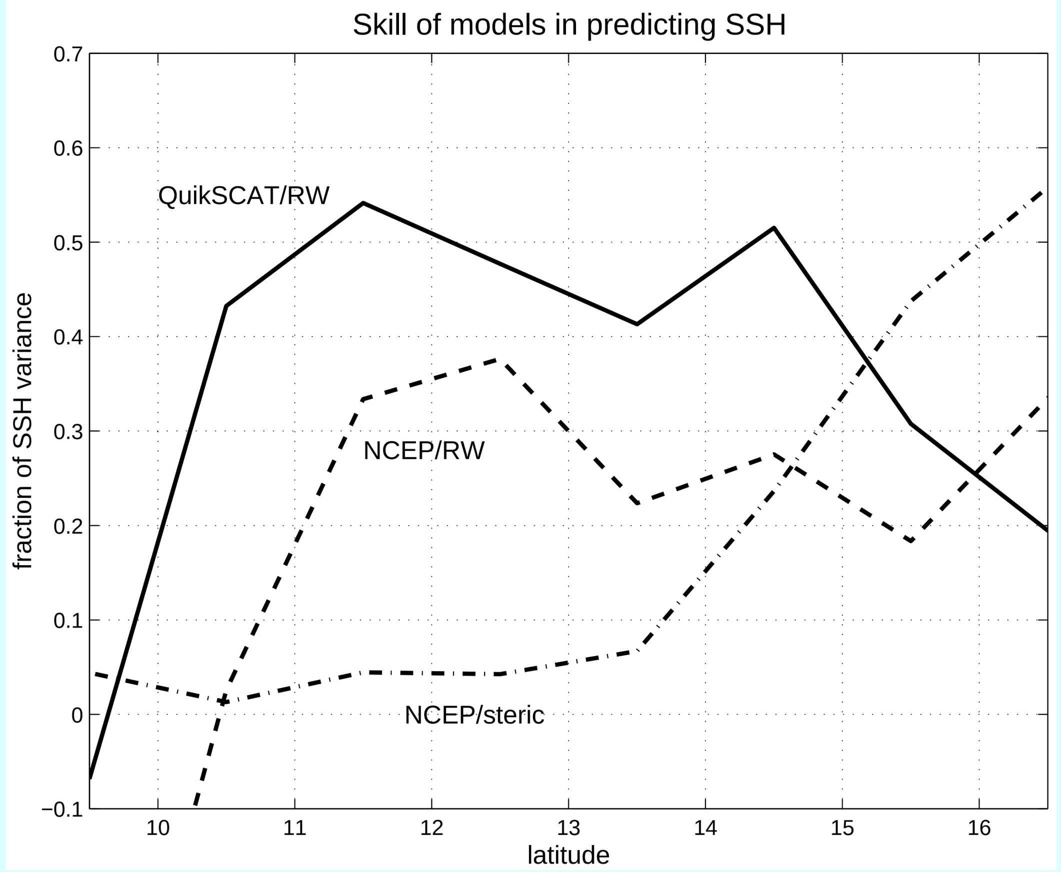

Figure 6. Skill of simple models in reproducing observed SSH anomalies. Fraction of observed variance described by the steric model with NCEP fluxes (dash-dot), the Rossby wave model with NCEP wind stress curl (dash), and with QuikSCAT curl (solid). Note the large improvement in the simulation of the SSH using QuikSCAT wind stress for the Rossby Wave (RW) model. North of 15˚N, the steric response dominates the SSH field.

Summary:

The observed SSH at 10-16˚N (Figure 1b) is dominated by zonal bands of anomalies, which were shown to be best described by the local response to wind-stress curl forcing (Figure 5). The dominant balance is between the first term on the left-hand-side and the forcing term on the right-hand-side of equation (2b), or local Ekman pumping. Westward propagation with a phase speed consistent with baroclinic Rossby waves is apparent, but is smaller than the local forcing (Figure 5c). That the dominance of local forcing results from the strength of the wind stress curl annual cycle, and *not from a damping* of the free Rossby waves is only apparent when the simple model is forced by the scatterometer wind fields. It is not necessary to invoke a damping mechanism to explain the weak Rossby wave propagation.

The errors in the NCEP fields relative to the QuikSCAT wind stress curl fields have several probable sources in this region. Numerical weather prediction models have consistently had trouble simulating the small spatial scales of the ITCZ region (Trenberth, et al., 1990). In addition, there is a fundamental difference between the scatterometer and model winds: the NWP model simulates the motion of the air, whereas the scatterometer measures relative motion (the vector difference between the air and ocean movement), which is what contributes to the stress. The difference between winds from QuikSCAT and from anemometers on the Tropical-Atmosphere Ocean (TAO) moorings was shown to clearly match the measured ocean currents in the TAO array and to contribute large differences in the wind stress curl (Kelly, et al., 2001). The North Equatorial Countercurrent, which has a distinct annual cycle, is contained within the study region (10-16˚N) and may contribute to differences in the QuikSCAT curl.

References

Gill, A.E., and P.P. Niiler, The theory of the seasonal variability in the ocean, *Deep Sea Res.*, **20**, 141-177, 1973.

Kessler, W. S., Observations of long Rossby waves in the northern tropical Pacific, *J. Geophys. Res.*, **95**, 5183-5217, 1990.

Kelly, K. A., S. Dickinson, M. J. McPhaden, and G. C. Johnson, Ocean currents evident in satellite wind data, *Geophys. Res. Lett.*, **28**, 2469-2472, 2001.

Meyers, G., On the annual Rossby wave in the tropical north Pacific Ocean, *J. Phys. Oceanogr.*, **9**, 663-674, 1979.

Stammer, D., Steric and wind-induced changes in TOPEX/POSEIDON large-scale sea surface topography observations, *J. Geophys. Res.*, **102**, 20,987-21,009, 1997.

Trenberth, K.E., W.G. Large, and J.G. Olson, The mean annual cycle in global wind stress, *J. Phys. Oceanogr.*, **20**, 1742-1760, 1990.